

LLAMAS: A Facility Integral Field Spectrograph for the Magellan Telescopes

PI: R. Simcoe; Co-Is: Gabor Furesz, Michael McDonald (MIT)

1. Overview

The Large Lenslet Array Magellan Spectrograph (LLAMAS) is an Integral Field Unit (IFU) spectrograph being planned as a facility instrument for the 6.5-meter Magellan Telescopes. LLAMAS uses a densely packed microlens+fiber array and replicated low-cost spectrographs to deliver 2560 optical spectra ($R=1300$, $\lambda=350-970\text{nm}$) filling a $40'' \times 36''$ celestial solid angle. The microlens architecture can accommodate an increased field size (up to $60'' \times 60''$; 7680 fibers) as an option for expansion. The spatial pitch of $0.75''$ is matched to Magellan's excellent site seeing (median $0.7''$). LLAMAS has a uniquely powerful combination of etendue, spectral coverage, fill factor, and observational duty cycle.

The US astronomy community has invested heavily in multi-wavelength survey telescopes to mine the sky with unprecedented depth in the next decade. Many of these facilities (e.g. LSST, SPT-3G, ALMA) are located in the Southern Hemisphere, and are therefore geographically coincident with Magellan. However the community lacks a concerted strategy for spectroscopy and astrophysical characterization of the thousands of sources these facilities will uncover.

LLAMAS is designed for highly efficient observation of explosive astrophysical transients and blind survey fields with a solid angle matched to (a) the angular size of galaxy clusters at $z=1$, (b) the extent of circumgalactic gas envelopes at $z > 0.5$, and (c) the ALMA primary beam at 300 Ghz. Combining Magellan's aperture with complete simultaneous optical coverage, LLAMAS will enable deep exploration of distant and faint phenomena, complementing observations of the local universe made with existing IFUs on smaller telescopes.

2. Target Science

LLAMAS is envisioned as a facility instrument and so will be available for any program, and to any investigators with Magellan access. Its design was developed using requirements flowdown based on several specific applications briefly summarized below.

Design Parameter	LLAMAS (MRI scope)	LLAMAS (Full scope)
Lenslet pitch	0.75"	0.75"
Lenslet fill factor	$\geq 93\%$	$\geq 93\%$
Field of View (MRI Scope)	$40'' \times 36''$	$60'' \times 60''$
Wavelength Coverage	360-970 nm	360-970 nm
Spectral Resolution	$R = 1300$	$R = 1300$
Red / Blue Dichroic split	570 nm	570 nm
Telescope port	Aux Nasmyth (between elev. bearings)	Aux Nasmyth (between elev. bearings)
Availability	365 nights / year	365 nights / year
Sensors	Two 2048x2048, red deep depl.	Two 2048x2048, red deep depl.
Modes	Full frame, nod-and-shuffle	Full frame, nod-and-shuffle
Fiber run	4.5 meters Polymicro FPBI	4.5 meters Polymicro FPBI
# Spectrographs	8	24
# Fibers	2560	7680

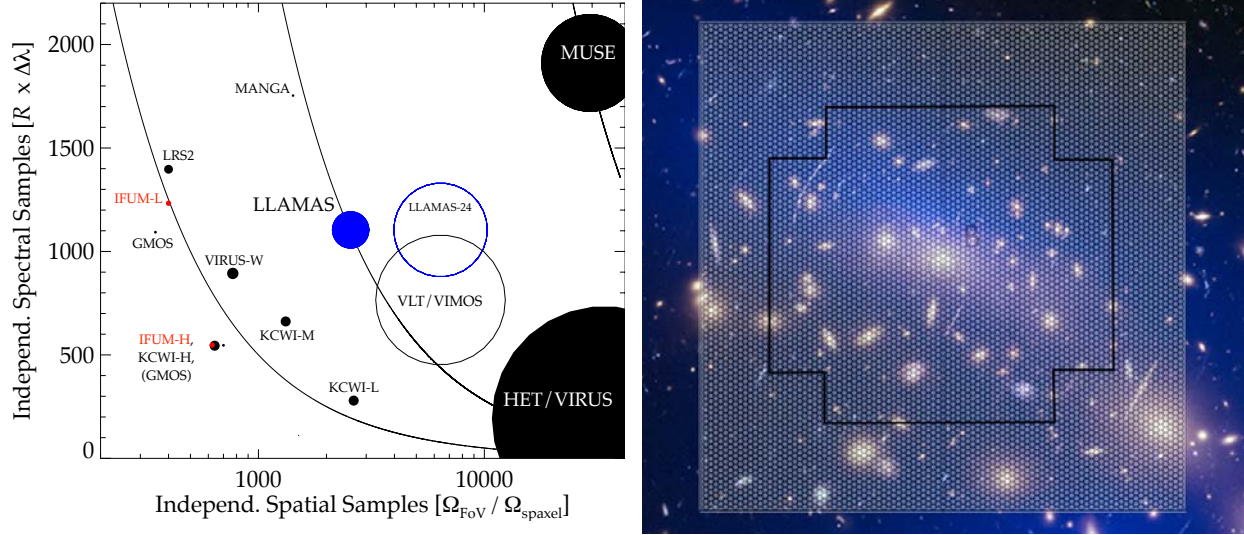


Figure 1: *Left:* Information grasp of selected existing or planned IFUs, indicating the number of independent spatial samples and spectral samples for each. Symbol sizes denote instrumental etendue with contours of constant information content. LLAMAS would provide the US with a deep, wide-field survey IFU in the Southern hemisphere. *Right:* HST image of a low-redshift galaxy cluster with overlay of the LLAMAS micro-lens array (MLA), indicating the field of view and sampling. The MLA can accommodate a $60'' \times 60''$ field. We proposed in 2017 MRI to populate the inscribed $40'' \times 36''$ region, as required for the science programs in 2.1-2.3.

2.1. Physics and Classification of LSST Transients

Efficient spectrographs on large-aperture, southern telescopes are essential to maximize the scientific return of LSST and its counterparts. As a Facility Instrument LLAMAS will be mounted on the telescope 365 days per year and accessible for either rapid followup of Targets of Opportunity, or queued observations during fractionally scheduled nights. LLAMAS $f = 93\%$ sky filling factor and large FoV obviate the need for time-consuming target acquisition, enabling rapid or scripted harvesting of spectra by service observers for later offline analysis. At $R=1300$ LLAMAS easily resolves the broad features characteristic of explosive transients. Its broad bandpass captures key spectral features across a wide redshift range, and simultaneously obtains spectra of associated host galaxies.

2.2. Southern SZ Cluster Surveys and Astrophysics

With the launch of eRosita, and the completion of two Stage-3 CMB experiments (SPT-3G, Advanced ACTpol), the number of known galaxy clusters will soon increase by orders of magnitude, particularly at $z > 1$. Despite these advances, pure SZ experiments cannot measure cluster redshifts, limiting their usefulness for cosmological and astrophysical studies. This problem is particularly acute at high redshift where the red sequence (used to estimate photometric redshifts of clusters) is not yet well-formed, so clusters blend with the field in color space. LLAMAS' large field of view and wavelength coverage will facilitate measurement of [OII] redshifts, velocity dispersions, and cooling radiation in young clusters in a single pointing on the SZ decrement centroid.

2.3. Gas Flows in the Circumgalactic Medium

The primary bottleneck in studying the high- z CGM is identifying large galaxy samples in projected proximity to bright background QSOs, whose absorption spectra probe the metallicity and kinematics of foreground CGM envelopes. Blue-sensitive, wide-field IFUs are optimal for overcoming this obstacle, because: (a) the characteristic radius of CGM metal-line absorption is ~ 120 kpc, or $15''$, (b) the strongest spectroscopic features, particularly Ly α , fall in the UV at $z > 2$, requiring spectroscopy at 3600\AA , and (c) galaxies can be targeted without *a priori* photometric identification.

LLAMAS is designed explicitly for observation of the $z = 2-3$ CGM, complementing the capabilities of

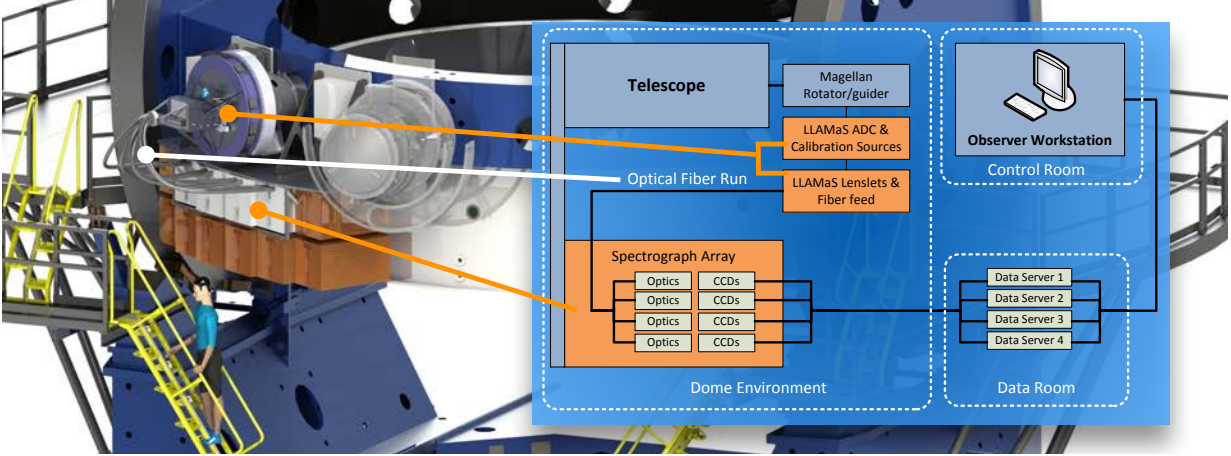


Figure 2: System architecture of LLAMAS and associated mechanical assembly as mounted permanently on the Magellan Folded Port. The four white cabinets below the FP contain the eight spectrographs imaging $40'' \times 36''$ as proposed here. These slew vertically upward with telescope elevation angle but do not rotate with position angle. Eight additional transparent orange cabinets illustrate envelope of the full $60'' \times 60''$ configuration. A short fiber run, protected by braided steel conduit, preserves high blue throughput.

VLT./MUSE by extending toward bluer wavelengths that cover Ly α at this epoch and benefit from the $(1+z)^4$ scaling in surface brightness. These redshifts encompass the peak era of star formation, black hole growth, and baryonic accretion. They also offer an increased surface density of galaxies and bright background QSOs, improving the chance of fortuitous small-separation pairs that trace the inner CGM.

LLAMAS also balances KCWI, in part by covering the Southern sky, but also through increased field of view ($2.2\times$ larger at equivalent R , or $4.4\times$ for KCWI's $R=3000$ mode) and wavelength coverage (until completion of KCWI-R). LLAMAS' increased FoV allows single-pointing coverage of the full CGM volume, and its simultaneous spectral coverage of OIII] $\lambda\lambda 1661, 1666\text{\AA}$, HeII $\lambda 1640\text{\AA}$ and CIII] $\lambda 1909\text{\AA}$ will trace massive stars and may help identify reionization-era analog galaxies at intermediate redshifts.

3. Instrument Design

The LLAMAS IFU employs a lenslet-fed fiberoptic bundle mounted at Magellan's Auxiliary Nasmyth focus. The fiber bundle runs to a bank of eight replicated spectrometers bolted to the telescope structure (Figure 2). The decision to mount at a FP is driven by the requirements of rapid response and high up-time for transient science.

3.1. Lenslet Array / Fiber Plug Plate

LLAMAS uses a biconvex micro-lens array (MLA) fabricated of fused silica to slice the Magellan focal plane into $0.75''$ spatial elements (Figure 3). The MLA projects a pupil onto the face of each $110\mu\text{m}$ diameter fiber, while also converting Magellan's native F/11 beam to an effective F/4.4 ray bundle, which is needed to meet our focal ratio degradation (FRD) loss specification of $< 5\%$. We successfully fabricated a run of prototype MLAs for the full $60'' \times 60''$ field of view as part of our early program development.

The fibers are aligned to high precision with the MLA by bonding into a pre-fabricated "Fiber Plug Plate" (FPP), which is also on a fused silica substrate, manufactured through photo-assisted chemical etching. This process preserves micron-level alignment over wide temperature ranges, since the MLA and FPP are thermally matched and bonded together during laboratory alignment. We also contracted a fabrication run of FPPs, matched to our as-built MLAs, as part of prototyping efforts (Figure 4). We have tested procedures for fiber preparation (stripping and cleaving), and built a workstation for insertion and bonding of fibers into the FPP (Figure 5).

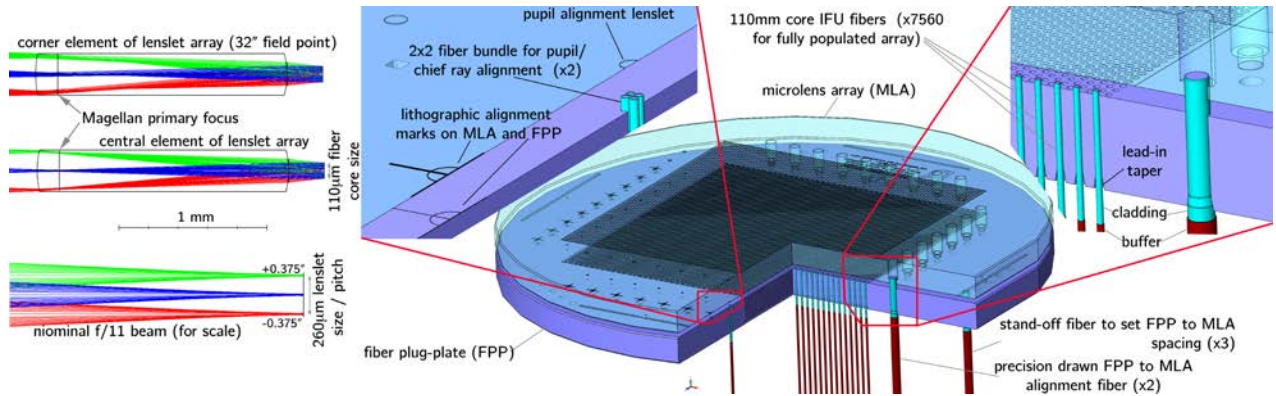


Figure 3: *Left:* Optical ray trace of a lenslet on the boresight (center) and array corner (top) showing the extent of the ray bundle on the fiber pupil, and the minimal departure from telecentric condition. *Right:* solid model of the lenslet array / plug plate assembly. In addition to the small-diameter science fibers, the assembly has numerous optical alignment markings, precision-drawn fibers for mechanical registration of the plug plate and lenslets, and a 2x2 fiber chief ray alignment bundle for adjusting the IFU’s tilt at the telescope focal plane.

3.2. Fiber Run

To preserve high blue throughput, the fiber run traverses only 4.5 meters from the focal plane to the spectrograph bank, which is attached to the telescope elevation ring (Figure 2). The fibers are standard round-core Polymicro FBPI, with ends prepared by plasma stripping and carefully controlled cleaving. We have constructed an FRD measurement station for quality control during fiber handling; using this apparatus we have verified that cleaved and unpolished fibers repeatably meet our FRD specification of >95% transmission of the F/4.4 beam at the fiber input into the F/4.0 acceptance cone of the collimator. The fibers are protected in braided steel conduit, and emerge into a fused silica “blade” that forms the pseudo-slit in the spectrograph. The slit is curved and tilts the individual fibers to minimize aberrations introduced by the spherical reflecting spectrograph collimator.

3.3. Spectrograph Optics

Figure 6 shows the optical layout of a single LLAMAS spectrograph, developed in response to the following requirements:

- Passband: High sensitivity from $\lambda=350\text{nm}$ (goal 30% at 360nm for Ly α at $z = 2$) to 950nm (to cover

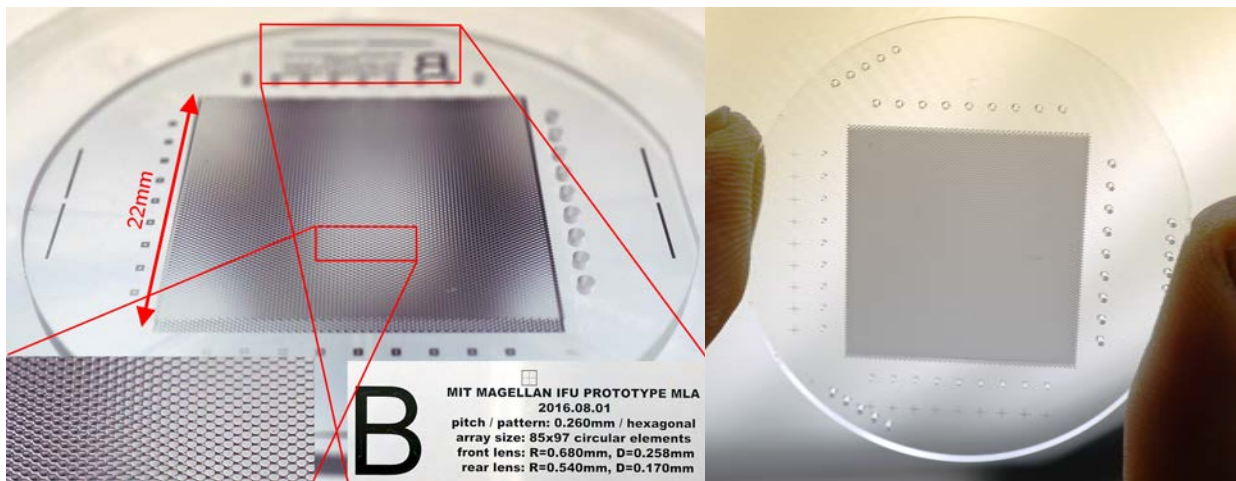


Figure 4: (left) Photo of the 60''x60'' prototype biconvex MLA successfully manufactured during prototyping. (Right) Photo of the corresponding fiber plug plate, also manufactured during prototype engineering. We have multiple copies of each substrate, reducing schedule and technical risk for the project.

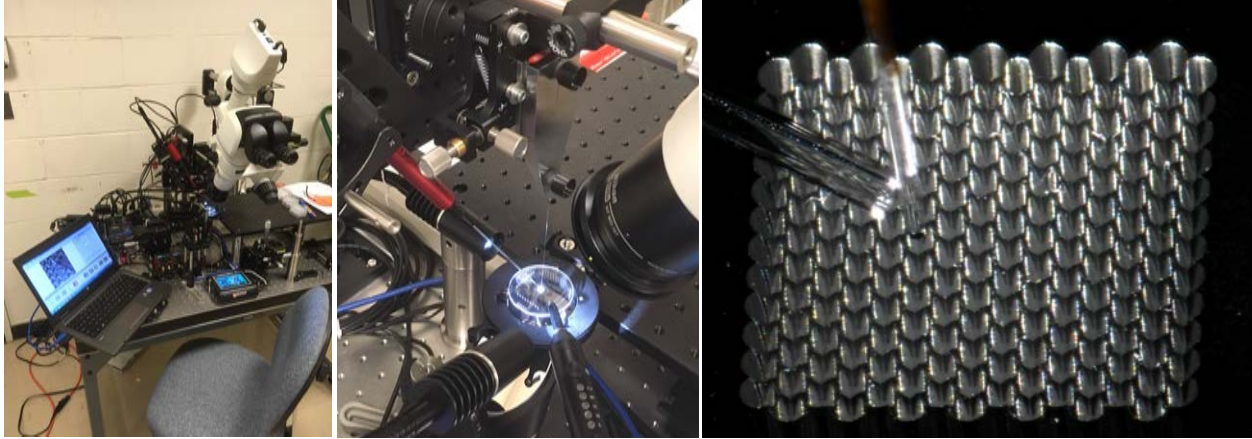


Figure 5: Fiber bonding workstation, including close-up (center) illustrating a fiber being bonded into our prototype plug plate. The fiber is inserted from above and bonded using micro-pipetted epoxy (red cylinder). A UV curing lamp flashes the bond once inspection from the microscope (right) verifies proper epoxy application.

the Balmer break in $z \sim 1$ clusters), and capture the full optical band pass in a single exposure for rapid ToO classification.

- Spectral Resolution: Resolve the Mg II $\lambda 2800\text{\AA}$ (750 km/s) and C IV $\lambda 1550$ (480 km/s) doublets (requirement) and marginally resolve [OII] $\lambda 3727$ (217 km/s).
- Blue / Red Channels: To preserve high throughput over a factor of 2.7 in wavelength and limit sensor costs, split by a dichroic into red and blue channels that are dispersed by separate Volume Phase Holographic (VPH) gratings and imaged by optimized cameras.
- Pseudo-slit parameters: 110 μm round-core fibers to match the scientifically-motivated sky pitch and F/4.4 input of the MLA. The fibers shall project >95% of rays into the F/4.0 beam of the collimator, averaged over the slit (10% FRD equivalent).

The spectrograph collimator is simple on-axis $f = 200\text{mm}$ sphere, with field curvature and coma minimized by the geometry of the pseudo-slit. Its 50mm parallel beam is split by a dichroic at 570nm and projected through separate VPH gratings into red and blue cameras. The 7-element cameras are all-spherical with F/1.4 and $f = 90\text{mm}$.

3.4. Spectrograph Mechanics

The individual spectrographs, which each accommodate 320 fibers, mount to either side of a carbon fiber optical bench which bolts to the side of the telescope. For the 40" x 36" LLAMAS build, this requires eight spectrographs, bundled into four pairs. We align and assemble the camera optics separately

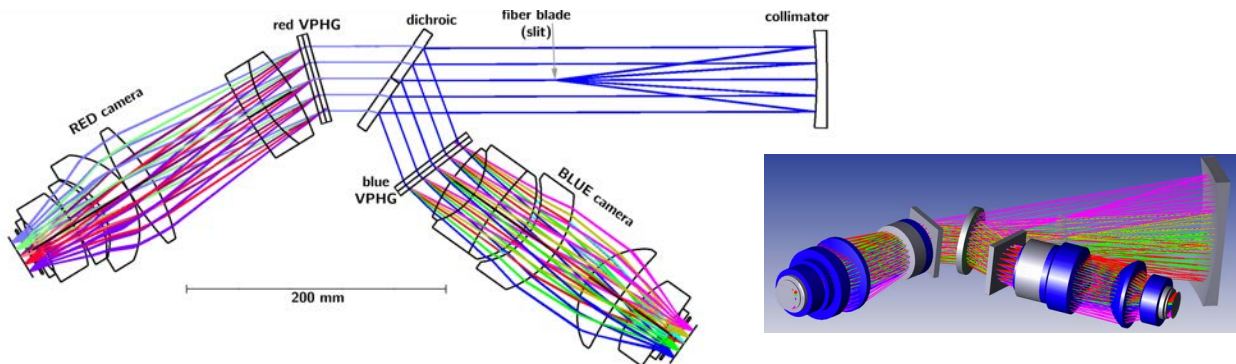


Figure 6: Optical layout of LLAMAS' spectrograph, showing red/blue division (left) and collimator pupil (inset)

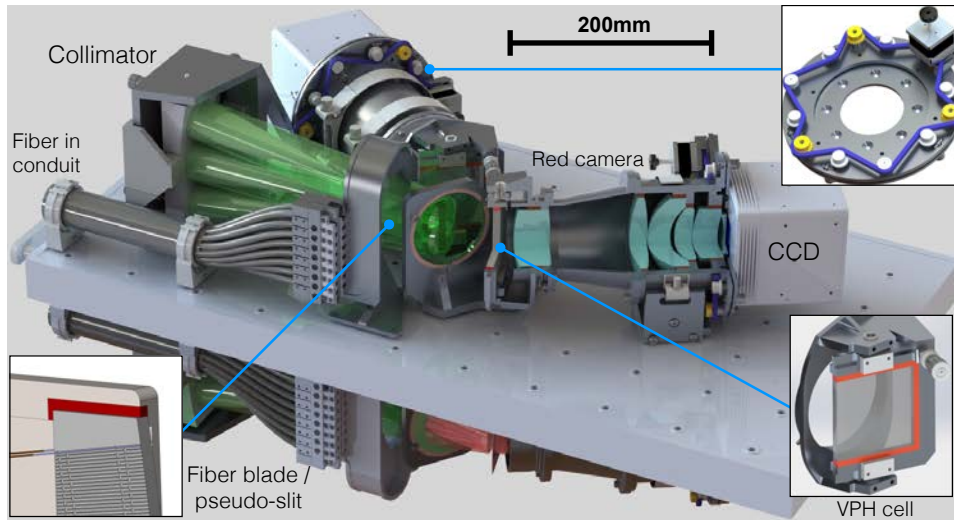


Figure 7: Solid model rendering of one 2-spectrograph unit, illustrating mirror symmetry across the carbon fiber bench, input fiber conduits, pupil location of the collimator, and division into red and blue channels with Raptor CCD camera heads. Insets show mechanisms, including individual focus control of the F/1.4 spectrograph cameras.

using OptiCentric workstations at MIT Lincoln Labs and verify alignment interferometrically. The camera barrels are integrated with the CCD housings and bolted to the bench. The collimator is aligned interferometrically using kinematic adjustments. The spectrographs are mounted within a space frame on the telescope, with access provided by a sliding rail mechanism.

3.5. Detectors

Our baseline design employs 2048 x 2048 CCD42-40 sensors from E2V, packaged by a commercial vendor with integrated thermoelectric cooling. We have specified a configuration that permits bi-directional clocking for nod-and-shuffle operation. The CCDs for the red arm are budgeted as deep-depletion devices to minimize fringing.

3.6. Performance Projections

Figure 8 shows the projected optical performance of the spectrograph over varying combinations of wavelength and field angle seen at the detector. The simulated images at right indicate trace separation when all fibers area illuminated. For low background observations, an optional second mode is available with smaller FoV, but wider trace separation for detailed background estimation. Figure 9 indicates the projected throughput from the ADC to the focal plane, along with a visual indication of individual transmission losses from specific subsystems. The right panel illustrates tests of cleaved prototype fibers

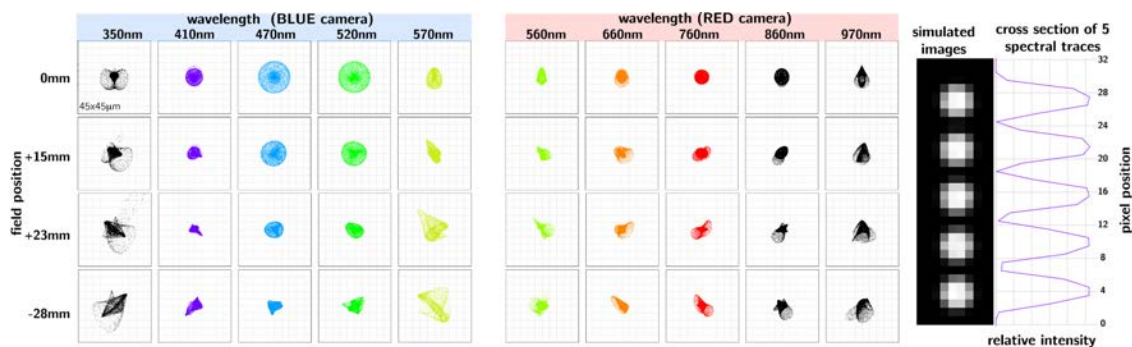


Figure 8: (Left) Spot diagrams illustrating spectrograph performance over all λ and field angles. Boxes are 45 x 45 microns, or approximately one resolution element. (Right): Arc-line profiles from our integrated instrument simulation (§C.8), illustrating inter-trace spacing and sampling. An alternate mode allows illumination of every second fiber for precision background subtraction.

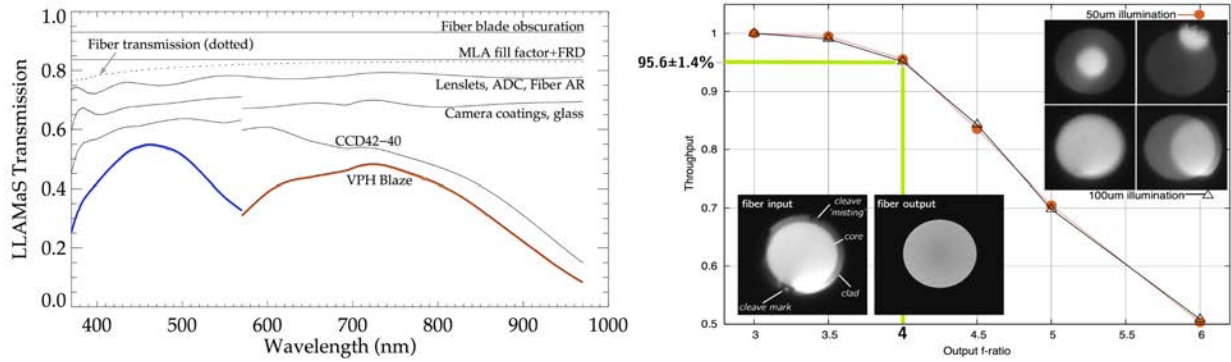


Figure 9: (Left) Projected LLAMAS throughput, with individual losses indicated. (Right): FRD test measurements for FBPI fibers processed in our strip/cleave station (without polishing). The fibers display improved surface roughness and flatness compared to polished ends, and meet our specification of projecting >95% of rays entering the fiber at F/4.4 into an F/4.0 output cone.

illustrating that our fiber process maintains FRD control at $95.6 \pm 1.4\%$ throughput for a 40-fiber lot. Finally Figure 10 shows a simulated 7-hour spectrum of a Lyman break galaxy at $r = 25.0$, using the throughput projections of Figure 9 together with a model of the telescope and atmosphere.

4. Program Development

We have applied to the 2017 NSF/MRI competition for funding to build eight spectrographs and populate the inner $40 \times 36''$ of the MLA. This will fulfill the baseline science requirements outlined in Section 2. We have also calculated marginal costs to populate the remaining portion of the array, should additional funding become available in the future for a larger survey instrument. The target date for first light is in 2020B, with commissioning complete in mid-2021.

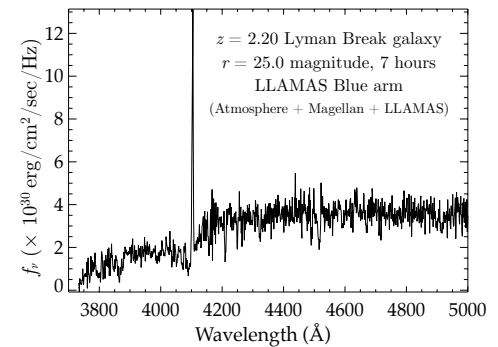


Figure 10: Simulated LLAMAS spectrum of a $z=2.2$ Lyman Break Galaxy, showing the strong sensitivity to Ly α emission and the Ly α forest decrement from LLAMAS blue throughput.

	LLAMAS		MUSE	KCWI	IFU-M	Manga	VIRUS
	MRI scope	Full scope					
Spatial sampling	0.75"	0.75"	0.20" x 0.65"	0.15" x 0.70" [0.15" x 1.4"]	0.63" or 1.25"	2.0"	1.5"
Field of view	40" x 36"	60" x 60"	60" x 60"	20" x 16.8" [20" x 32"]	15" x 14" or 25" x 21"	32"	275" x 275" (sparse pack)
Spectral R	1300	1300	1200-6200	4000 [2000]	2,000-40,000	2000	700
$\Delta\lambda$ (nm)	610 (350-960)	610 (350-960)	450 (480-930)	350 (350-700)	~20 @ R=20k 450 @ R=2k	640 (360-1000)	200 (350-550)
# Spatial resol. elements	2560	7360	~11,000	1440	624 or 400	1423	34,000
Telescope	Magellan (6.5m)	Magellan (6.5m)	VLT (8m)	Keck (10m)	Magellan (6.5m)	SDSS (2.5m)	HET (10m)
Availability (% nights)	100%	100%	≤ 50%	~40%	~5-10%	50%	50%